# Hydrothermal synthesis and crystal structure of $Cs_6[(UO_2)_4(W_5O_{21})(OH)_2(H_2O)_2]$: a new polar uranyl tungstate

Richard E. Sykora[*,1], Thomas E. Albrecht-Schmitt

*Department of Chemistry, Auburn University, Auburn, Alabama 36849, USA*

## Abstract

The hydrothermal reaction of $UO_3$, $WO_3$, and $CsIO_4$ leads to the formation of $Cs_6[(UO_2)_4(W_5O_{21})(OH)_2(H_2O)_2]$ and $UO_2(IO_3)_2(H_2O)$. $Cs_6[(UO_2)_4(W_5O_{21})(OH)_2(H_2O)_2]$ is the first example of a hydrothermally synthesized uranyl tungstate. It's structure has been determined by single-crystal X-ray diffraction. Crystallographic data: tetragonal, space group $I4cm$, $a = 15.959(2)$ Å, $c = 14.215(1)$ Å, $Z = 4$, Mo$K\alpha$, $\lambda = 0.71073$ Å, $R(F) = 2.84\%$ for 135 parameters with 2300 reflections with $I > 2\sigma(I)$. The structure is comprised of two-dimensional $_{\infty}^{2}[(UO_2)_4(W_5O_{21})(OH)_2(H_2O)_2]^{6-}$ anionic layers that are separated by $Cs^+$ cations. The coordination polyhedra found in the novel layers consist of $UO_7$ pentagonal bipyramids, $WO_6$ distorted octahedra, and $WO_5$ square pyramids. The $UO_7$ polyhedra are formed from the binding of five equatorial oxygen atoms around a central uranyl, $UO_2^{2+}$, unit. Both bridging and terminal oxo ligands are employed in forming the $WO_5$ square pyramidal units, while oxo, hydroxo, and aqua ligands are found in the $WO_6$ distorted octahedra. In the layers, four $(UO_2)O_5$ polyhedra corner share with equatorial oxygen atoms to form a $U_4O_{24}$ tetramer entity with a square site in the center; a tungsten atom populates the center of each of these sites to form a $U_4WO_{25}$ pentamer unit. The pentamer units that result are connected in two dimensions by edge-shared dimers of $WO_6$ octahedra to form the two-dimensional $_{\infty}^{2}[(UO_2)_4(W_5O_{21})(OH)_2(H_2O)_2]^{6-}$ layers. The lack of inversion symmetry in $Cs_6[(UO_2)_4(W_5O_{21})(OH)_2(H_2O)_2]$ can be directly contributed to the $WO_5$ square pyramids found in the pentamer units. In the structure, all of these polar polyhedra align their terminal oxygens in the same orientation, along the $c$ axis, thus resulting in a polar compound.
© 2004 Elsevier Inc. All rights reserved.

*Keywords:* Hydrothermal synthesis; Single-crystal X-ray diffraction; Uranyl tungstate; Layered compound

## 1. Introduction

The solid-state chemistry of uranyl inorganic phases and minerals has received a significant attention lately due to the possibility of their formation during the storage of spent nuclear fuel. In particular, the incorporation of the oxoanions of elements with radioactive isotopes present in spent nuclear fuel [1], including [129]I [2–7], [181]W [8–11], [79]Se [12–15], and [93]Mo [16–23], into uranyl structures has gained focus. In this regard, a number of uranyl tungstates have been prepared in high-temperature solid-state reactions and display a rich structural chemistry because of variability in both the uranyl and tungsten coordination [8–11]. In known uranyl compounds, tungsten can have tetrahedral coordination as found in $Na_{10}[(UO_2)_8(W_5O_{20})O_8]$ [9] and $UO_2WO_4$ [24,25]. The five- and six-coordinate modes for tungsten polyhedra that have been seen in uranyl compounds are illustrated in the structures of $M_2[(UO_2)(W_2O_8)]$ ($M =$ Li, Na, K, Ag) [8–10], $M_2[(UO_2)_2(WO_5)O]$ ($M =$ K, Rb) [9], and $Li_2[(UO_2)_4(WO_4)_4O]$ [8]; coordination polyhedra of Mo(VI) show similarities to tungsten polyhedra and can also be four-, five-, or six-coordinate [16–25].

Earlier work on the incorporation of uranyl groups into polyoxotungstates found that several anions could be isolated both in solution and the solid state [26,27].

---

*Corresponding author. Fax: +865-574-4987.

*E-mail address:* sykorare@ornl.gov (R.E. Sykora).

[1]Current location is Chemical Sciences Division, Oak Ridge National Laboratory, Post Office Box 2008, Mail Stop, MS 6375, Oak Ridge, TN 37831-6375, USA.

The reaction of $UO_2^{2+}$ with $[NaAs_4W_{40}O_{140}]^{27-}$ can produce $[(UO_2)_3(H_2O)_5As_3W_{29}O_{104}]^{19-}$ or $[(UO_2)_3(H_2O)_6As_3W_{30}O_{105}]^{15-}$, depending on the reaction conditions, of which the ammonium salts have been characterized by single crystal X-ray diffraction [26]. Single crystal structural analysis as well as $^{31}P$ and $^{183}W$ NMR have been used to characterize the sodium, ammonium, and potassium salts of $[M_2(UO_2)_2(PW_9O_{34})_2]^{12-}$ ($M$ = Na, $NH_4$, K) [27]. The neptunyl, $NpO_2^+$, derivative of the latter complex anion has also been formed with sodium [28] and the extraction behavior of both the uranyl and neptunyl derivatives have been studied [27,28].

Using hydrothermal synthesis our group has recently prepared, and structurally characterized using single-crystal X-ray diffraction, a number of uranium oxides containing both main-group and transition-metal anions in the form of uranyl iodates [2–5], periodates [6,7], selenites [12–14], and chromates [19,29,30] such as: $UO_2(IO_3)_2(H_2O)$ [5], $K_2[(UO_2)_2(VO)_2(IO_6)_2O]\cdot H_2O$ [7], $A[(UO_2)_3(HIO_6)_2(OH)(O)(H_2O)]\cdot 1.5H_2O$ ($A$ = Li, Na, K, Rb, Cs) [6], $[C_4H_{12}N_2]_{0.5}[UO_2(HSeO_3)(SeO_3)]$ [14], and $K_6[(UO_2)_4(CrO_4)_7]\cdot 6H_2O$ [29]. In addition, we have recently reported the single-crystal structure of the first hydrothermally produced uranyl antimonite, $UO_2Sb_2O_4$ [31]. Herein we report the synthesis and single-crystal structure of a novel uranyl tungstate, $Cs_6[(UO_2)_4(W_5O_{21})(OH)_2(H_2O)_2]$.

# 2. Experimental

## 2.1. Syntheses

$UO_3$ (99.8%, Alfa-Aesar), $WO_3$ (99.998%, Alfa-Aesar), $Cs_2CO_3$ (99%, Alfa-Aesar), CsOH (99.9%, Alfa-Aesar), and $H_5IO_6$ (98%, Alfa-Aesar) were used as received. $CsIO_4$ was prepared from the reaction of $Cs_2CO_3$ and $H_5IO_6$ as reported by de Waal et al. [32]. Distilled and millipore filtered water with a resistance of $18.2\,M\Omega$ was used in all reactions. Reactions were run in Parr 4749 23-mL autoclaves with PTFE liners. The reaction reported produced the highest yield of the desired compound. SEM/EDX analyses were performed using a JEOL 840/ Link Isis instrument. U and W percentages were calibrated against standards. Typical results are within 3% of actual ratios. *Warning: While the $UO_3$ contains depleted U, standard precautions for handling radioactive materials should be followed. Old sources of depleted U should not be used, as the daughter elements of natural decay are highly radioactive and present serious health risks.*

## 2.2. $Cs_6[(UO_2)_4(W_5O_{21})(OH)_2(H_2O)_2]$

$UO_3$ (184 mg, 0.644 mmol), $WO_3$ (149 mg, 0.644 mmol), and $CsIO_4$ (417 mg, 1.29 mmol) were loaded in a 23-mL PTFE-lined autoclave, 1.7 M CsOH (0.5 mL) was then added to the solids. The autoclave was sealed and placed in a box furnace and then heated to 180 °C where the reaction occurred under autogenously generated pressure. After 72 h the furnace was cooled at 9 °C/h to 23 °C. The product mixture included yellow blocks of $Cs_6[(UO_2)_4(W_5O_{21})(OH)_2(H_2O)_2]$ and yellow crystals of $UO_2(IO_3)_2(H_2O)$ [5] as well as a mixture of other unidentified yellow and colorless products beneath a pale yellow mother liquor. The mother liquor was decanted from the products, which were then washed with water, followed by methanol, and allowed to dry. The yellow crystals of $Cs_6[(UO_2)_4(W_5O_{21})(OH)_2(H_2O)_2]$ were the minor product, and could visually be separated from the other products. EDX analysis for $Cs_6[(UO_2)_4(W_5O_{21})(OH)_2(H_2O)_2]$ provided a Cs:U:W ratio of 6:4:5.

## 2.3. Crystallographic studies

A single crystal of $Cs_6[(UO_2)_4(W_5O_{21})(OH)_2(H_2O)_2]$ with dimensions of $0.070 \times 0.070 \times 0.064\,mm^3$ was mounted on a glass fiber with epoxy and aligned on a Bruker SMART APEX CCD X-ray diffractometer with a digital camera. An Oxford Cryostat was used to adjust the data collection temperature to –80 °C. Intensity measurements were performed using graphite monochromated Mo $K\alpha$ radiation from a sealed tube with a monocapillary collimator. SMART was used to determine the preliminary cell constants from 90 frames collected with an exposure time of 10 s, and to subsequently control the data collection. The intensities of reflections of a sphere were collected by a combination of three sets of exposures (frames). Each set had a different $\varphi$ angle for the crystal and each exposure covered a range of $0.3°$ in $\omega$. A total of 1800 frames were collected with an exposure time per frame of 30 s.

Determination of integrated intensities and global cell refinement were performed with the Bruker SAINT (v 6.02) software package using a narrow-frame integration algorithm. An analytical absorption correction was applied, followed by a semi-empirical absorption correction using SADABS [33,34]. The program suite SHELXTL (v 5.1) was used for space group determination (XPREP), direct methods structure solution (XS), and least-squares refinement (XL) [35]. The final refinement included anisotropic displacement parameters for all atoms. Some crystallographic details are listed in Table 1 and the final positional parameters for $Cs_6[(UO_2)_4(W_5O_{21})(OH)_2(H_2O)_2]$ can be found in Table 2. Further details of the crystal structure investigation may be obtained from the Fachinformation-

Table 1
Crystallographic data for $Cs_6[(UO_2)_4(W_5O_{21})(OH)_2(H_2O)_2]$

| Formula | $Cs_6[(UO_2)_4(W_5O_{21})(OH)_2(H_2O)_2]$ |
|---|---|
| Formula mass | 3202.88 |
| Color and habit | Yellow, block |
| Space group | $I4cm$ |
| $a$ (Å) | 15.959(2) |
| $c$ (Å) | 14.215(1) |
| $V$ (Å$^3$) | 3620.5(6) |
| $Z$ | 4 |
| $T$ (°C) | −80 |
| $\lambda$ (Å) | 0.71073 |
| Maximum $2\theta$ (deg) | 56.60 |
| Observed data $I > 2\sigma(I)$ | 2300 |
| $\rho_{calcd}$ (g cm$^{-3}$) | 5.865 |
| $\mu$(Mo $K\alpha$) (cm$^{-1}$) | 396.80 |
| Residual electron density (e Å$^{-3}$) | −2.751–2.651 |
| $R(F)$ for $F_o^2 > 2\sigma(F_o^2)$[a] | 0.0283 |
| $R_w(F_o^2)$[b] | 0.0658 |

[a] $R(F) = \sum ||F_o| - |F_c|| / \sum |F_o|$.
[b] $R_w(F_o^2) = \left[ \sum \left[ w(F_o^2 - F_c^2)^2 \right] / \sum wF_o^4 \right]^{1/2}$.

Table 2
Atomic coordinates and equivalent isotropic displacement parameters for $Cs_6[(UO_2)_4(W_5O_{21})(OH)_2(H_2O)_2]$

| Atom | Ref. Occ[a] | $x$ | $y$ | $z$ | $U_{eq}$ (Å$^2$)[b] |
|---|---|---|---|---|---|
| Cs(1) | | 0.3628(1) | 0.3369(1) | 0.0428(1) | 0.020(1) |
| Cs(2) | 0.443(6) | 0.5704(2) | 0.0704(2) | 0.4187(3) | 0.050(1) |
| Cs(3) | 0.390(18) | 0.0969(3) | 0.4031(3) | 0.0629(17) | 0.069(6) |
| Cs(4) | 0.287(17) | 0.0891(3) | 0.4109(3) | 0.1182(7) | 0.023(2) |
| U(1) | | 0.4905(1) | 0.2954(1) | 0.3002(1) | 0.013(1) |
| W(1) | | $\frac{1}{2}$ | $\frac{1}{2}$ | 0.3728(1) | 0.013(1) |
| W(2) | | 0.3659(1) | 0.1341(1) | 0.2280(1) | 0.015(1) |
| W(3) | | 0.2281(1) | 0.2719(1) | 0.2894(1) | 0.025(1) |
| O(1) | | 0.4239(5) | 0.5831(6) | 0.3335(7) | 0.020(2) |
| O(2) | | $\frac{1}{2}$ | $\frac{1}{2}$ | 0.4948(14) | 0.021(4) |
| O(3) | | 0.4753(6) | 0.1535(6) | 0.2554(7) | 0.022(2) |
| O(4) | | 0.3530(5) | 0.2553(5) | 0.2605(6) | 0.015(2) |
| O(5) | | 0.3634(7) | 0.1366(7) | 0.1075(12) | 0.030(4) |
| O(6) | | 0.3722(11) | 0.1278(11) | 0.3995(18) | 0.066(7) |
| O(7) | | 0.2449(6) | 0.3798(5) | 0.3225(7) | 0.022(2) |
| O(8) | | 0.2634(6) | 0.2366(6) | 0.4202(8) | 0.013(2) |
| O(9) | | 0.2104(7) | 0.2896(7) | 0.1632(11) | 0.027(3) |
| O(10) | | 0.4751(5) | 0.2742(6) | 0.4231(7) | 0.017(2) |
| O(11) | | 0.5082(6) | 0.3189(7) | 0.1781(6) | 0.018(2) |

[a] Refined Occupancy, See text for constrained occupancies.
[b] $U_{eq}$ is defined as one-third of the trace of the orthogonalized $U_{ij}$ tensor.

The absolute structure parameter, which is the fractional contribution of the inverted component of a racemic twin [36], for $Cs_6[(UO_2)_4(W_5O_{21})(OH)_2(H_2O)_2]$ is 0.35(1). This implies that the crystal that was investigated is a racemic twin, and the data was refined as such. In addition, the Cs(2), Cs(3), and Cs(4) sites were found to be only partially occupied with refined occupancies of 0.443(6), 0.390(18), and 0.287(17), respectively. The occupancies for the Cs positions were set based on the results when the occupancies were allowed to vary in the early stages of refinement; the occupancy for Cs(2) was set at 0.5 and the sum of the occupancies for Cs(3) and Cs(4) positions were constrained, because of their close proximity (0.806(17) Å), to a value of 0.5.

## 3. Results and discussion

### 3.1. Syntheses

The hydrothermal reaction of $UO_3$, $WO_3$, and $CsIO_4$ in 1.7 M CsOH solution has led to the production of a new uranyl tungstate, $Cs_6[(UO_2)_4(W_5O_{21})(OH)_2(H_2O)_2]$. While $Cs_6[(UO_2)_4(W_5O_{21})(OH)_2(H_2O)_2]$ does not incorporate any form of iodate anions, periodate or iodate, into its structure, as determined from semi-quantitative X-ray analysis (EDX), direct reactions of $UO_3$, $WO_3$, and CsOH under similar reaction conditions have not been successful in producing $Cs_6[(UO_2)_4(W_5O_{21})(OH)_2(H_2O)_2]$. Although the role of the periodate in the reaction has not been determined conclusively, the formation of the $UO_2(IO_3)_2(H_2O)$ [5] byproduct reveals that at least part of the periodate is reduced to iodate in the reaction, as is the case in most hydrothermal reactions involving periodate. However, past reports have discussed that compounds containing periodate, $Ba_3[(MoO_2)_2(IO_6)_2] \cdot 2H_2O$ [37] and $K_2[(UO_2)_2(VO)_2(IO_6)_2O] \cdot H_2O$ [7], can be isolated under similar basic conditions as employed for these reactions.

The production of $Cs_6[(UO_2)_4(W_5O_{21})(OH)_2(H_2O)_2]$ has proven to be highly sensitive to reaction duration, pH, and reaction composition. In some cases, multiple reactions had to be run under identical conditions to ensure its formation. The formation of $UO_2(IO_3)_2(H_2O)$ [5] is one factor that impedes the production of $Cs_6[(UO_2)_4(W_5O_{21})(OH)_2(H_2O)_2]$ as also found in the production of $Cs_2[UO_2(CrO_4)(IO_3)_2]$ [30]. Similar synthetic challenges have been reported for $BaMo_2O_5(SeO_3)_2$ and $BaMoO_3SeO_3$, where $BaMo_4O_{13} \cdot 2H_2O$ was obtained in many regions of compositional space [38].

### 3.2. Structure

The structure of $Cs_6[(UO_2)_4(W_5O_{21})(OH)_2(H_2O)_2]$ contains two-dimensional anionic layers, as do the majority of U(VI) structures [39], separated and charge-balanced by cesium cations. The $^2_\infty[(UO_2)_4$
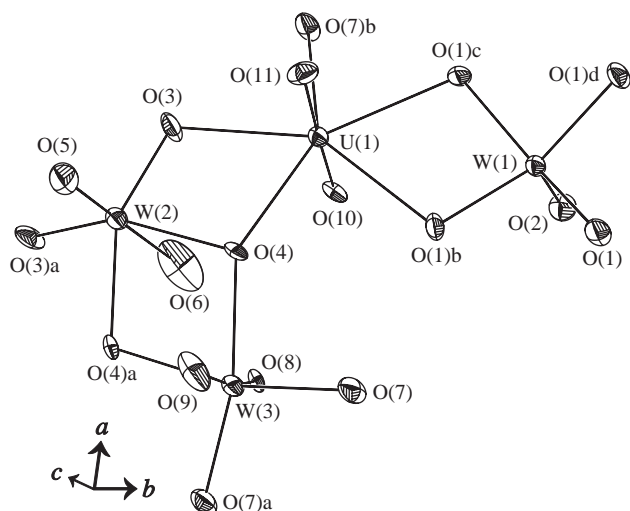
Fig. 1. A depiction of the local environments of U(1), W(1), W(2), and W(3) in $Cs_6[(UO_2)_4(W_5O_{21})(OH)_2(H_2O)_2]$, 50% probability ellipsoids are shown.



Fig. 2. A ball-and-stick representation of the two-dimensional, anionic $^2_\infty[(UO_2)_4(W_5O_{21})(OH)_2(H_2O)_2]^{6-}$ layers in $Cs_6[(UO_2)_4(W_5O_{21})(OH)_2(H_2O)_2]$.

$(W_5O_{21})(OH)_2(H_2O)_2]^{6-}$ layers found in $Cs_6[(UO_2)_4(W_5O_{21})(OH)_2(H_2O)_2]$ contain three types of polyhedral building units: $UO_7$ pentagonal bipyramids, $WO_6$ distorted octahedra, and $WO_5$ square pyramids. The $UO_7$ polyhedra are formed from the binding of five equatorial oxygens around a nearly linear central uranyl, $UO_2^{2+}$, unit. Both bridging and terminal oxo ligands are employed in forming the $WO_5$ square pyramidal units, while oxo, hydroxo, and aqua ligands are found in the two crystallographically unique $WO_6$ distorted octahedra. A thermal ellipsoid plot (Fig. 1) of the anionic structural building unit displays the co-ordination environments for the uranium and tungsten atoms.

In the layers, four $(UO_2)O_5$ uranium polyhedra corner share with equatorial oxygen atoms to form a $U_4O_{24}$ tetramer entity with a square site in the center. Each site is occupied with a tungsten atom, W(1), in square pyramidal coordination, to form a $U_4WO_{25}$ pentamer unit. The pentamers of polyhedra that result are connected in two dimensions by edge-shared dimers of $WO_6$ octahedra to form the two-dimensional $^2_\infty[(UO_2)_4(W_5O_{21})(OH)_2(H_2O)_2]^{6-}$ layers as shown in Figs. 2 and 3 with ball-and-stick and polyhedral representations, respectively. These anionic layers stack in the crystallographic (ab) plane and the interlayer spacing is one-half of the c-axis or ~7.14 Å. Cesium cations are found between the layers. They serve to balance charge as well as ionically bond the layers together with $Cs^+$–O ionic contacts. A packing diagram for $Cs_6[(UO_2)_4(W_5O_{21})(OH)_2(H_2O)_2]$, showing the anionic layers separated by $Cs^+$ cations is shown in Fig. 4.

An interesting feature of $Cs_6[(UO_2)_4(W_5O_{21})(OH)_2(H_2O)_2]$ is its lack of inversion symmetry, since the majority of U(VI) structures are centrosymmetric [39],
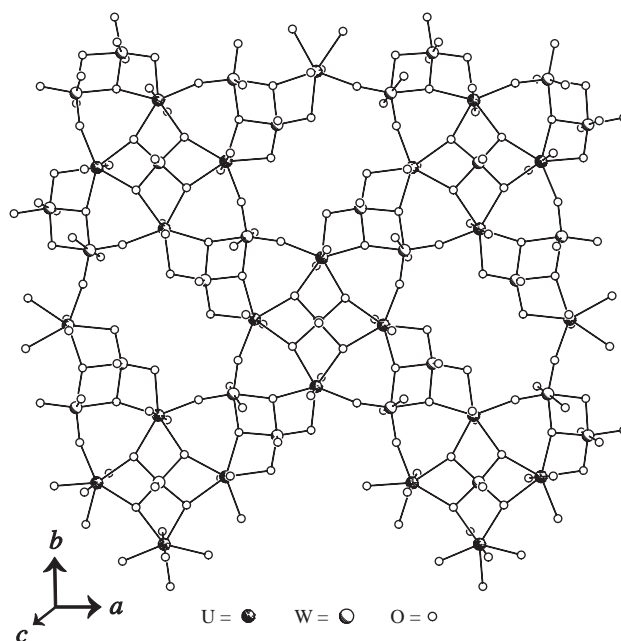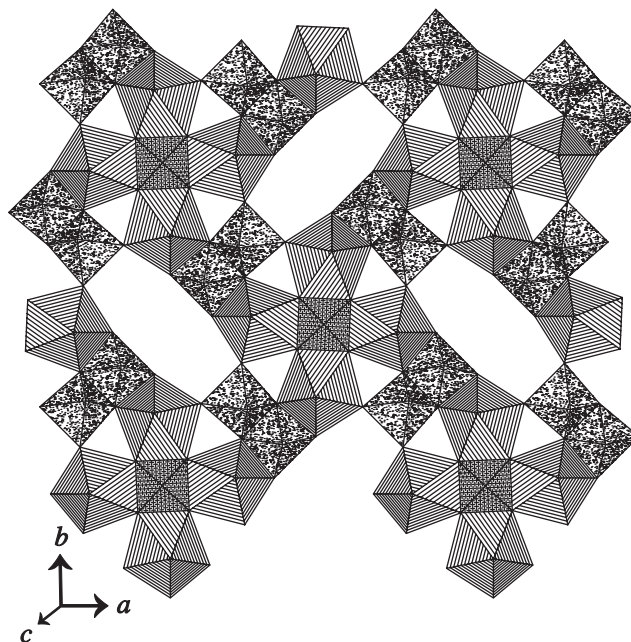


Fig. 3. A polyhedral representation of the $^2_\infty[(UO_2)_4(W_5O_{21})(OH)_2(H_2O)_2]^{6-}$ layers in $Cs_6[(UO_2)_4(W_5O_{21})(OH)_2(H_2O)_2]$. The coordination polyhedra shown in the layers consist of $UO_7$ pentagonal bipyramids (parallel lines), $WO_6$ distorted octahedra (random dot pattern), and $WO_5$ square pyramids (herringbone).

as are all of the uranyl tungstates that have been structurally characterized previously [8–10]. The trans uranyl unit, $UO_2^{2+}$, that is generally found in U(VI) compounds can easily be placed on an inversion center
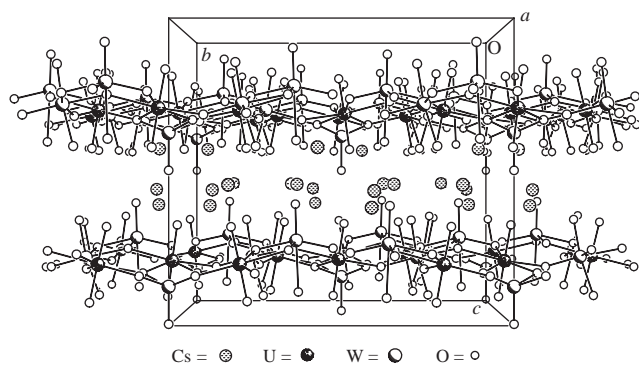
Fig. 4. A view of the stacking of the $^{2}_{\infty}[(UO_2)_4(W_5O_{21})(OH)_2(H_2O)_2]^{6-}$ layers in $Cs_6[(UO_2)_4(W_5O_{21})(OH)_2(H_2O)_2]$. $Cs^+$ cations are located between the layers.

Table 3
Selected bond distances (Å) for $Cs_6[(UO_2)_4(W_5O_{21})(OH)_2(H_2O)_2]$

Distances (Å)

| | | | |
|---|---|---|---|
| U(1)–O(1)b | 2.411(9) | W(2)–O(3) | 1.815(9) |
| U(1)–O(1)c | 2.418(9) | W(2)–O(3)a | 1.815(9) |
| U(1)–O(3) | 2.366(9) | W(2)–O(4) | 1.999(9) |
| U(1)–O(4) | 2.355(8) | W(2)–O(4)a | 1.999(9) |
| U(1)–O(7)b | 2.243(8) | W(2)–O(5) | 1.714(17) |
| U(1)–O(10) | 1.797(9) | W(2)–O(6) | 2.44(3) |
| U(1)–O(11) | 1.797(9) | W(3)–O(4) | 2.052(8) |
| W(1)–O(1) | 1.883(9) | W(3)–O(4)a | 2.052(8) |
| W(1)–O(1)b | 1.883(9) | W(3)–O(7) | 1.806(9) |
| W(1)–O(1)c | 1.883(9) | W(3)–O(7)a | 1.806(9) |
| W(1)–O(1)d | 1.883(9) | W(3)–O(8) | 2.022(12) |
| W(1)–O(2) | 1.73(2) | W(3)–O(9) | 1.838(15) |

Symmetry codes: (a) $0.5-y$, $0.5-x$, $z$; (b) $1-y$, $x$, $z$; (c) $1-x$, $1-y$, $z$; (d) $y$, $1-x$, $z$.

Table 4
Bond valence sums for atoms in $Cs_6[(UO_2)_4(W_5O_{21})(OH)_2(H_2O)_2]$

Bond valence sum

| | | | |
|---|---|---|---|
| U(1) | 5.98 | O(7) | 2.04 |
| W(1) | 6.11 | O(8) | 0.76 |
| W(2) | 6.28 | O(9) | 1.25 |
| W(3) | 6.15 | O(10) | 1.63 |
| O(1) | 2.08 | O(11) | 1.63 |
| O(2) | 1.68 | Cs(1) | 1.36 |
| O(3) | 1.86 | Cs(2) | 1.02 |
| O(4) | 2.06 | Cs(3) | 1.47 |
| O(5) | 1.74 | Cs(4) | 0.84 |
| O(6) | 0.25 | | |

and normally precludes the formation of noncentro-symmetric (NCS) compounds. In $Cs_6[(UO_2)_4(W_5O_{21})(OH)_2(H_2O)_2]$, the lack of inversion can be directly contributed to the $WO_5$ square pyramids. In the structure, all of these polar anions align their terminal oxygens in the same orientation, along the $c$-axis, thus resulting in a NCS and polar compound.

The bond lengths and angles for the uranium polyhedra are within expected limits for pentagonal bipyramidal coordination. U–O distances of 1.797(9) Å are found for the uranyl unit, while the O–U–O angle is nearly linear with a value of 178.4(5)°. The equatorial oxygen atoms are nearly perpendicular to the uranyl unit as expected for U(VI) compounds, with distances and angles ranging from 2.243(8) Å to 2.418(9) Å and 63.6(4)° to 79.9(3)°, respectively. The W(1) atomic position has a square pyramidal coordination formed from the coordination of four bridging oxygen atoms at its base with distances of 1.883(9) Å and one short terminal oxygen bound at its apex (W–O distance of 1.73(2) Å). Both W(2) and W(3) atomic positions are coordinated by six oxygen atoms in distorted octahedral coordination environments. W–O bonds to oxide, hydroxide, and aqua ligands are found, which are reflected in the wide range of bond lengths, varying from 1.714(17) to 2.44(3) Å. The water molecule is assigned as the O(6) position based on the W(3)–O(6) bond length of 2.44(3) Å [40]. Based on bond length and bond valence sum calculations (Table 4) O(8) is likely the position of the hydroxo unit. Additional bond lengths for $Cs_6[(UO_2)_4(W_5O_{21})(OH)_2(H_2O)_2]$ can be found in Table 3.

The bond valence sum for uranium has been calculated using the values given by Burns et al. for pentagonal bipyramidal coordination and it has a value of 5.98, consistent with U(VI) [41]. For W(1), W(2), and W(3), the calculated bond valence sums are 6.11, 6.28, and 6.15, respectively [42]. Bond valence sums for the remaining atoms have been calculated [42] and can be found in Table 4.

### 3.3. Structural relationships

In the known structures of previously reported uranyl tungstates [8–10], the uranium coordination has been almost exclusively pentagonal bipyramidal as found in $Cs_6[(UO_2)_4(W_5O_{21})(OH)_2(H_2O)_2]$ and the majority of other U(VI) structures [39]; one noted exception is the presence of tetragonal bipyramidal coordination of uranium, along with pentagonal bipyramidal coordination, in the structure of $Li_2[(UO_2)_4(WO_4)_4O]$ [8]. The coordination of the tungsten centers has shown more variation. Four-, five-, and six-coordinate tungsten polyhedra have all been discovered in uranyl tungstates with geometries including tetrahedral, square-pyramidal, tetragonal pyramidal, and distorted octahedral. $M_2[(UO_2)_2(WO_5)O]$ ($M$ = K, Rb) [9] contain both square- and tetragonal-pyramidal tungsten coordination, where these polyhedra are each coordinated to five uranium pentagonal bipyramids through corner- and edge-sharing. The square pyramids observed in $Cs_6[(UO_2)_4(W_5O_{21})(OH)_2(H_2O)_2]$ are much more regular; all of the basal oxygens are equidistant from the tungsten center and four equivalent edge sharing

interactions to four uranyl polyhedra are present (Fig. 3). Octahedral coordination of tungsten is the most prevalent in uranyl tungstate structures, as it has been found in $M_2[(UO_2)W_2O_8]$ ($M$ = Li, Na, $\alpha$-Ag, $\beta$-Ag, K) [8–10], $Na_{10}[(UO_2)_8(W_5O_{20})O_8]$ [9], and $Li_2[(UO_2)_4(WO_4)_4O$ [8], as well as reported here for $Cs_6[(UO_2)_4(W_5O_{21})(OH)_2(H_2O)_2]$. $M_2[(UO_2)W_2O_8]$ ($M$ = Na, $\alpha$-Ag, $\beta$-Ag, K) [9,10] contain one-dimensional $(W_2O_8)$ chains formed from both corner- and edge-shared tungsten octahedra, while $Na_{10}[(UO_2)_8(W_5O_{20})O_8]$ [9] contains five-member tungsten oxide clusters containing four distorted octahedra and one tetrahedron. The first isolated dimers of tungsten polyhedra in uranyl tungstates are seen in $Cs_6[(UO_2)_4(W_5O_{21})(OH)_2(H_2O)_2]$, where they serve to connect the isolated $[U_4WO_{25}]$ pentamers (Fig. 3). A similar pentamer unit formed with $(UO_2)O_5$ uranium polyhedra and a five coordinate molybdenum polyhedron has been isolated in $K_8(UO_2)_8(MoO_5)_3O_6$ [23].

# Acknowledgment

# References

[1] J. C. Tait, I. C. Gauld, G. B. Wilkin, AECL-9881.
[2] R.E. Sykora, A.C. Bean, B.L. Scott, W. Runde, T.E. Albrecht-Schmitt, J. Solid State Chem. 177 (2004) 725.
[3] T. Y. Shvareva, P. M. Almond, T. E. Albrecht-Schmitt, J. Solid State Chem. 2004, submitted for publication.
[4] A.C. Bean, C.F. Campana, O. Kwon, T.E. Albrecht-Schmitt, J. Am. Chem. Soc. 123 (2001) 8806.
[5] A.C. Bean, S.M. Peper, T.E. Albrecht-Schmitt, Chem. Mater. 13 (2001) 1266.
[6] T.A. Sullens, R.A. Jensen, T.Y. Shvareva, T.E. Albrecht-Schmitt, J. Am. Chem. Soc. 126 (2004) 2676.
[7] R.E. Sykora, T.E. Albrecht-Schmitt, Inorg. Chem. 42 (2003) 2179.
[8] S. Obbade, S. Yagoubi, C. Dion, M. Saadi, F. Abraham, J. Solid State Chem. 177 (2004) 1681.
[9] S. Obbade, S. Yagoubi, C. Dion, E. Bekaert, S. Yagoubi, M. Saadi, F. Abraham, J. Solid State Chem. 172 (2003) 305.
[10] S.V. Krivovichev, P.C. Burns, Solid State Sci 5 (2003) 373.
[11] C. Askeljung, M. Sundberg, J. Solid State Chem. 144 (1999) 152.
[12] P.M. Almond, S.M. Peper, E. Bakker, T.E. Albrecht-Schmitt, J. Solid State Chem. 168 (2002) 358.
[13] P.M. Almond, T.E. Albrecht-Schmitt, Inorg. Chem. 41 (2002) 1177.
[14] P.M. Almond, T.E. Albrecht-Schmitt, Inorg. Chem. 42 (2003) 5693.
[15] J. -C. Trombe, J. Galy, J. Solid State Chem. 61 (1986) 308.
[16] S.V. Krivovichev, P.C. Burns, Can. Mineral. 40 (2002) 1571.
[17] S.V. Krivovichev, P.C. Burns, Can. Mineral. 40 (2002) 201.
[18] S.V. Krivovichev, R.J. Finch, P.C. Burns, Can. Mineral. 40 (2002) 193.
[19] R.E. Sykora, S.M. McDaniel, D.M. Wells, T.E. Albrecht-Schmitt, Inorg. Chem. 41 (2002) 5126.
[20] S.V. Krivovichev, P.C. Burns, Can. Mineral. 39 (2001) 197.
[21] S.V. Krivovichev, P.C. Burns, Can. Mineral. 38 (2000) 717.
[22] S.V. Krivovichev, P.C. Burns, Can. Mineral. 38 (2000) 847.
[23] S. Obbade, S. Yagoubi, C. Dion, M. Saadi, F. Abraham, J. Solid State Chem. 174 (2003) 19.
[24] E.F. Juenke, S.F. Bartram, Acta Crystallogr 17 (1964) 618.
[25] V.N. Serezhkin, V.K. Trunov, L.G. Makarevich, Kristallografiya 25 (1980) 858.
[26] K.-C. Kim, M.T. Pope, J. Chem. Soc. Dalton Trans. (2001) 986.
[27] K. -C. Kim, M.T. Pope, J. Am. Chem. Soc. 121 (1999) 8512.
[28] A.J. Gaunt, I. May, M. Helliwell, S. Richardson, J. Am. Chem. Soc. 124 (2002) 13350.
[29] R.E. Sykora, S.M. McDaniel, T.E. Albrecht-Schmitt, J. Solid State Chem. 177 (2004) 1431.
[30] R.E. Sykora, D.M. Wells, T.E. Albrecht-Schmitt, Inorg. Chem. 41 (2002) 2304.
[31] R.E. Sykora, J.E. King, A.J. Illies, T.E. Albrecht-Schmitt, J. Solid State Chem. 177 (2004) 1717.
[32] D. de Waal, K. -J. Range, Z. Naturforsch. 51b (1996) 1365.
[33] R.H. Blessing, Acta Crystallogr. A 51 (1995) 33.
[34] F.Q. Huang, J.A. Ibers, Inorg. Chem. 40 (2001) 2602.
[35] G.M. Sheldrick, SHELXTL PC, Version 5.0, An Integrated System for Solving, Refining, and Displaying Crystal Structures from Diffraction Data, Siemens Analytical X-ray Instruments, Inc., Madison, WI, 1994.
[36] SHELXTL Reference Manual, v. 5.1, Bruker AXS, Inc., pp. 11–12. 1997.
[37] R.E. Sykora, D.M. Wells, T.E. Albrecht-Schmitt, Inorg. Chem. 41 (2002) 2697.
[38] W.T.A. Harrison, L.L. Dussack, A.J. Jacobson, J. Solid State Chem. 125 (1996) 234.
[39] P.C. Burns, M.L. Miller, R.C. Ewing, Can. Mineral. 34 (1996) 845.
[40] Y. Jeannin, C.R. Acad. Sci. Paris, Ser. IIc. 2 (1999) 161.
[41] P.C. Burns, R.C. Ewing, F.C. Hawthorne, Can. Mineral. 35 (1997) 1551.
[42] N.E. Brese, M. O'Keeffe, Acta Crystallogr. B 47 (1991) 192.